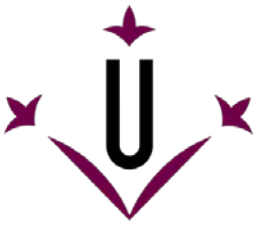

$MgSO_4 \cdot 7H_2O$ filled macro cellular foams: an innovative composite sorbent for thermo-chemical energy storage applications for solar buildings

Vincenza Brancato[1,*], Luigi Calabrese[1,2], Valeria Palomba[1], Andrea Frazzica[1], Margalida Fullana-Puig[3,4], Aran Solé[5], Luisa F. Cabeza[3]

[1]CNR – ITAE – Istituto di Tecnologie Avanzate per l'Energia "Nicola Giordano", Salita S. Lucia sopra Contesse 5, Messina 98126, Italy

[2]Department of Engineering, University of Messina, Messina, Italy

[3]GREiA Research Group, INSPIRES Research Centre, Universitat de Lleida, Pere de Cabrera s/n, 25001-Lleida, Spain

[4]CIRIAF-Interuniversity Research Centre on Pollution and Environment Mauro Felli, Via G. Duranti 63, 06125, Perugia, Italy

[5]Department of Mechanical Engineering and Construction, Universitat Jaume I, Campus del Riu Sec s/n, 12071 Castelló de la Plana, Spain

* Corresponding author: Vincenza Brancato. Email: vincenza.brancato@itae.cnr.it. Tel: +39 090 624243

Keywords: $MgSO_4 \cdot 7H_2O$, composite foams, thermochemical energy storage, sorption storage, salt hydrate, silicon based.

Abstract

For seasonal energy storage using solar energy in buildings heating and DHW, thermochemical technology represents the most promising alternative due to the virtually absence of heat losses during storage period. This work focuses on silicone foams, filled by $MgSO_4 \cdot 7H_2O$, as innovative composite sorbents for sorption thermal energy storage applications. The necessity to enclose the salt hydrate in the polymeric foam arises for overcoming the issue of swelling, agglomeration, and/or deliquescence of the salt during its de/hydration process. Indeed, the foam with its flexible structure allows the safe volume expansion during the hydration phase of the salt. The foam samples presented in this paper were obtained by mixing the salt hydrate at various percentages (from 40 wt.% up to 70 wt.%) with a mixture of two water vapour permeable silicones. The foams were characterized by a complete physicochemical and morphological examination in order to evaluate their actual application in sorption energy storage systems. It was demonstrated that a good link seems to be established between the foam and the salt, and that the de/hydration capacity of the salt is not hindered by the foaming process, storage ability and storage density of the composites are expected to be in line with those of the pure material.

1. Introduction

According to the International Energy Agency (IEA), space heating and cooling together with water heating account for about 60% of global energy consumption in buildings (International Energy Agency, 2013). This means that the heating and cooling in buildings represents the main sector in which it is possible to achieve relevant energy and Greenhouse gas (GHG) emission savings. Solar energy represents the most attractive solution to reduce the dependency on fossil fuels, especially for space heating and domestic hot water (DHW) production. In such a context, the roadmap of the Renewable Heating and Cooling platform identified as one of the priorities the development of Solar-Active-Houses (SAH), able to cover up to 60% of their energy demand by means of solar source (RHC European Technology Platform, 2014). A crucial technology to develop in order to achieve this goal is represented by the seasonal thermal energy storage (TES), able to provide heating energy during winter season by shifting the solar thermal energy harvested during summer season (Xu et al., 2014).

Different technologies are available for storage of solar energy, namely sensible heat, latent heat and thermochemical heat storage (Xu et al., 2014). However, for seasonal energy storage, thermochemical technology represents the most promising alternative, due to the virtually absence of heat losses during storage period. A growing interest has been recently devoted to thermochemical storage and thermochemical storage materials (TCMs), with the aim of synthetizing materials with high energy density and cycle stability for long-term operation (Aydin et al., 2015; Cabeza et al., 2017; Donkers et al., 2017).

Several classes of TCMs were evaluated, such as zeolites (Jänchen et al., 2004) and zeotypes (Yu et al., 2013), but among them, salt hydrates present outstanding properties, in terms of theoretical storage capacity in the range of temperatures of interest (<100°C), which can reach 3 GJ/m^3 (Donkers et al., 2017; Rammelberg et al., 2016). Nonetheless, their practical application still needs research efforts, in order to overcome different problems arising in the realisation of a storage system. Among them, the most critical are represented by the low thermal conductivity of the materials (Kleiner et al., 2017), that affect heat transfer, and the agglomeration and swelling phenomena, that limit vapour permeation, inducing degradation after cycling (De Jong et al., 2014; Donkers et al., 2016). In order to prevent such issues, the use of composites sorbents was proposed and currently represents a topic of great interest (Gordeeva and Aristov, 2012). This class of materials is based on two components: the host matrix and the inorganic salt placed inside the matrix pores. Several types of matrices and/or additives were proposed for application with salt hydrates, such as mesoporous materials, clays and carbonaceous structures (Xu et al., 2018; Zhao et al., 2016).

Whiting et al. (Whiting et al., 2013, 2014) and Hongois et al. (Hongois et al., 2011) used the wet impregnation method for the realisation of a $MgSO_4$ into different types of zeolites. Outcomes of the experimental campaigns carried out was that the form-stable composite represent a promising TCM for long-term storage purposes, thanks to their improved thermal properties, and thermal and chemical reliability. Posern et al. (Posern and Kaps, 2010) used wet impregnation technique on a mixture of $MgSO_4$ and $MgCl_2$ in

attapulgite matrices. Several studies on composites $CaCl_2$ are reported: investigated matrix and synthesis method include impregnation on iron silicate (Ristić and Henninger, 2014) and bentonite (Kerskes et al., 2010), impregnation in mesoporous silica gel (Courbon et al., 2017; Zhu et al., 2006) and synthesis in silica gel with the sol-gel method (Mrowiec-Białoń et al., 1997). Jabbari-Hichri et al. (Jabbari-Hichri et al., 2017) studied $CaCl_2$ with three different matrices: silica gel, alumina and bentonite showing that the best performance in terms of stored/released heat and water sorption capacity was obtained with the silica gel impregnated composite.

Recently, also different porous materials and structures were proposed. For instance, (Liu et al., 2015) developed a composite mesoporous honeycomb element based on Wakkanai siliceous shale (WSS) and lithium chloride (LiCl) for application in an open sorption thermal energy storage system, that showed good ciclability. Gaeini et al. (Gaeini et al., 2018) reported the comparison among composite sorbents employing calcium chloride as salt and different matrixes, namely, vermiculite, expanded graphite and a novel micro-encapsulation method based on ethyl cellulose, with high content of salt (>80%wt.). (Grekova et al., 2016) proposed the synthesis of composites with multi-wall carbon nanotubes embedding $CaCl_2$, LiCl and LiBr. Interestingly, they investigated not only water but also methanol as working fluid for closed sorption TES applications.

Generally, composites present enhanced properties with respect to the pure salts, in terms of thermal conductivity and chemical and physical stability. However, the major limit of the investigated matrixes is their rigid structure, which may suffer of long-term stability issues, due to the forces induced by the salt solution expansion during the hydration phase. Furthermore, the salt is usually confined into open pores, which are not able to keep the solution in case of oversaturation, causing a degradation of the composite itself. In this regards, polymeric foams can overcome most of the reported issues, since they present a flexible structure, allowing for the safe volume expansion during the hydration phase. Furthermore, some polymeric foams are permeable towards water vapour, allowing the vapour reacting also with salt confined inside closed porosity (Robb, 1968; Shui Wai Lin and Salvador Valera Lamas, 2011). This would inhibit the loss of salt solution in case of oversaturation. These features can be beneficial for the development of innovative composites with high energy storage density, thanks to the possibility of varying the pore size and pore volume, thus hosting relevant amount of salt. A similar approach has been successfully proposed for the realization of composites based on zeolites and polymeric foams for adsorption heat pump applications (Luigi Calabrese et al., 2017a, 2017b).

In the present work, a flexible composite for seasonal storage of solar energy is presented for the first time, consisting of silicone foams filled with $MgSO_4 \cdot 7H_2O$. Different foam samples were synthetized by mixing the salt hydrate at various percentages (from 40 wt.% up to 70 wt.%) with a mixture of two water vapour permeable silicones. The foams were then characterized by means of thermogravimetric measurement and FTIR analysis Foam morphology was evaluated by optical 3D digital microscope and scanning electron microscopy. Furthermore, the composition of the different phases was determined by energy dispersive

spectroscopy. Finally, the dehydration tests under closed sorption storage operating conditions were performed. In the next sections, the methodology used and the experimental results are detailed. Outcome of the study is that the composite show promising features for application in TES systems for solar energy.

2. Experimental Part

2.1. Foam synthesis

The concept of embedding an active filler inside a polymeric foam was recently proposed for adsorption heat pump applications, where the silicone foam was holding zeolite powders, to obtain a sorbent composite with high porosity and adsorption capacity (Luigi Calabrese et al., 2017b). In the present study, a mixture of poly(methylhydrosiloxane) $(CH_3(H)SiO)_n$ (code: PDMS) and a silanol terminated polydimethylsiloxane (code: PMHS) with proper catalyst was employed to form a polymeric foam that represents the hosting matrix for a salt hydrate ($MgSO_4 \cdot 7H_2O$) characterized by an excellent sorption capacity. The polymers were chosen for their high permeability to water vapour, in order to not affect the water vapour diffusion during the real operating conditions. Figure 1 shows schematically the sequence of the preparation steps of the salt-silicone foams.

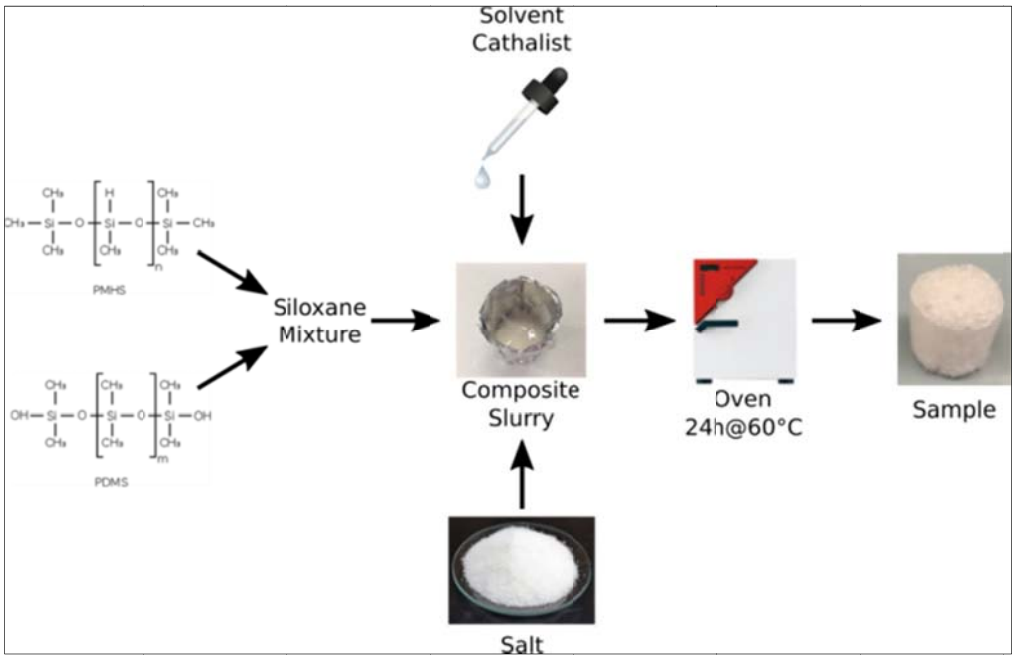

Figure 1. Flow chart of preparation phases of the salt-silicone foams

During the raw components mixing, the $MgSO_4 \cdot 7H_2O$ was dispersed in different percentages, and then the foaming process under controlled temperature was performed. The detailed synthesis process to obtain the foam is described in (L. Calabrese et al., 2017). Foamed salt-silicone structure is obtained by a joint action of crosslinking and foaming reactions of the siloxane constituents. The foaming expansion is caused by a

combination of a chemical blowing due to hydrogen evolution following the reaction among siloxane compounds and a physical blowing due to evaporation of the solvent, caused by heat release during the exothermic reaction. The reaction occurring during the sample synthesis is the following (Luigi Calabrese et al., 2017b):

$$\equiv Si - OH + H - Si \equiv \xrightarrow{Sn(II)} \equiv Si - O - Si \equiv \ + H_2 \uparrow$$

The reaction was promoted by the presence of the catalyst (Sn(II) compound). The new siloxane linkages formed in this reaction led to a rubber-like silicone network. Gaseous volatile products formed in the crosslinking reactions acted as blowing agents. Consequently, the crosslinking and the chemical foaming reactions progress simultaneously generating a well structured cellular foam (Calabrese et al., 2018). In Figure 2, the obtained foam samples with salt content varying from 40 wt.% up to 70 wt.% are presented.
The studied foams are categorized in the paper with the code "FOAM" followed by a number, which identifies the percentage of the salt added to the polymer matrix. For instance, the code "FOAM0" indicates the sample of the pure polymer matrix, while the code "FOAM50" indicates the sample made with 50% of salt hydrate.

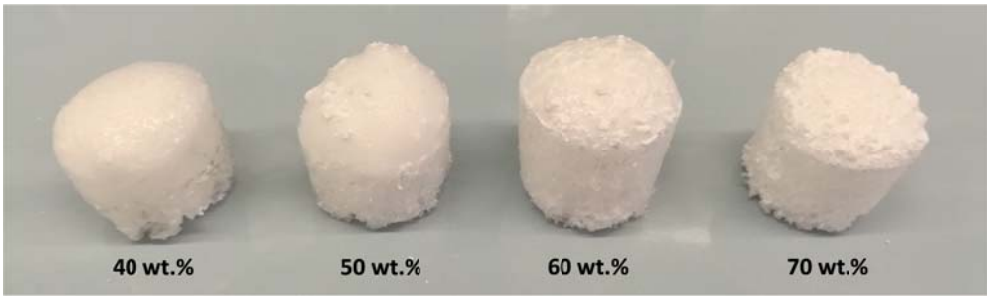

Figure 2. Prepared composite samples with different $MgSO_4 \cdot 7H_2O$ content

2.2. Constituent and foam characterization

Firstly, the main constituents of the polymer composites, namely the salt hydrate $MgSO_4 \cdot 7H_2O$ and the siloxane compounds, were characterized by means of thermogravimetric measurement and IR-spectroscopy, in order to evaluate their stability and their chemical properties. FTIR analysis was carried out using a Cary 670 Agilent spectrometer. The spectra were recorded from 500 to 4000 cm^{-1} on KBr based pellets. Thermogravimetric analysis was carried out by Netzsch Thermische Analyse TASC 414/2 performing a heating ramp between 25°C and 300°C with a heating rate of 1°C/min under nitrogen flow (50 ml/min).

A complete physicochemical and morphological characterization was performed on the polymer composite foams. The bulk density was computed by dividing the weight of the foam by its apparent volume. Both thermogravimetric analyses and FTIR test were repeated on the foams, following the same procedure used for the pure salt. Foam morphology was evaluated by optical 3D digital microscope (Hirox HK-8700). All the images were captured at 50x magnification. Morphological analysis was also performed by scanning

electron microscopy (SEM-FIB Zeiss Cross Beam 540). Furthermore, the composition of the different phases was determined by energy dispersive spectroscopy (EDS) (Aztec Oxford).

In order to assess the ability of the synthetized foam-salt composites to properly react with water vapour under typical working conditions, thermo-gravimetric dehydration tests were performed by means of a modified Labsys Evo SETARAM apparatus, whose main features are reported in the literature (Frazzica et al., 2014). The tests were performed as follows: the sample was weighted in an external microbalance, and then loaded inside the TG apparatus. Evacuation was performed at room temperature, down to 1 10^{-3} mbar. Afterwards, water vapour generated by an evaporator at 20°C was admitted in the testing chamber creating a pure water vapour atmosphere at 23.4 mbar. Subsequently, a heating ramp from 30°C up to 150°C was performed to evaluate the amount of water exchanged under these conditions. For each sample, three different specimens were extracted and tested, in order to take into account also possible inhomogeneity of the prepared samples.

3. Results and discussion

3.1. Salt hydrate and matrix characterization

Figure 3(a-c) shows the typical spectrum of $MgSO_4 \cdot 7H_2O$ salt and siloxane compounds, used in the composite foams, as filler and matrix, respectively.

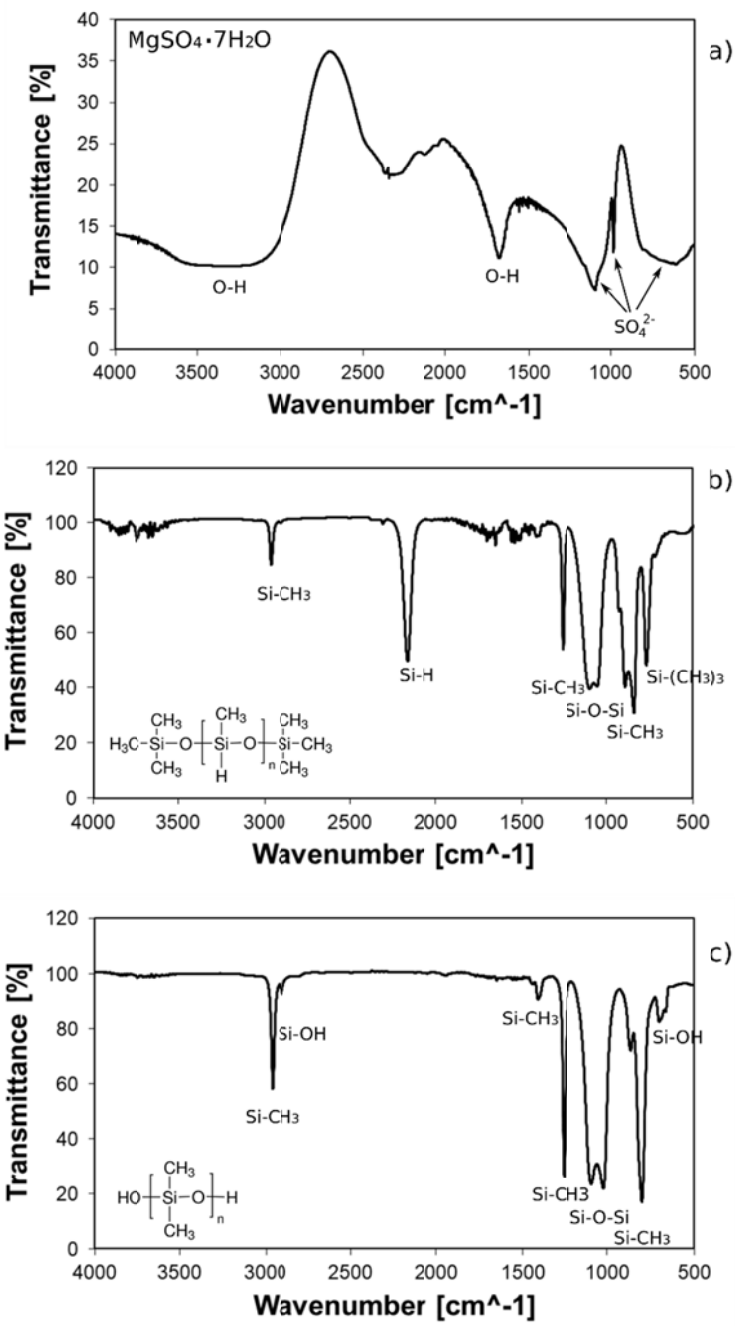

Figure 3. FTIR spectra: (a) $MgSO_4 \cdot 7H_2O$; (b) PMHS compound; (c) PDMS compound

FTIR spectrum of the magnesium sulphate salt shows a number of characteristic peaks: the broad peak in the range band 3500-3000 cm^{-1} indicates the presence of water while, the large peak at 1675 cm^{-1} can be assigned to bending modes of hydroxyl groups from intracrystalline water (Genceli et al., 2007). Furthermore, a large and very intense peak at about 1090 cm^{-1} and some less evident peaks at 980 cm^{-1} and 650-610 cm^{-1} were identified. These peaks are related to the vibrations of SO_4 bond: asymmetric stretching, symmetric stretching and bending, respectively (Ramalingom et al., 2003; Silverstein et al., 2005). PDMS and PMHS compounds spectra are characterized by absorption peaks typical for methyl groups, Si-CH_3 (2960, 1420, 1260 and 1255, 875-800 cm^{-1}) and siloxane groups, Si-O-Si (in the range band 1010-1110 cm^{-1}) (Miao et al., 2016). A relevant difference can be identified at ~2160 cm^{-1} where PMHS compound shows a

peak related to stretching vibrations of its reactive Si-H group. Of course, this peak was not observed in PDMS compound, that showed instead two well defined peaks at 2910 cm^{-1} and 680 cm^{-1} that can be related to stretching and bending of Si-OH groups, respectively (Luigi Calabrese et al., 2017b).

Thermal analysis was used to obtain information about both the dehydration of the pure salt hydrate and the stability of the polymeric matrix in a large range of temperatures. The results of the TG measurements are reported in Figure 4(a-b). TGA curves of the cross-linked PDMS and PMHS compounds show a small weight loss (-5.45%) in the temperature range 25-300°C (Figure 4a). In order to better evaluate the mass loss at increasing temperature, also the first derivate of TG-signal (DTG) was reported in Figure 4b. Hosseini et al. (Hosseini and Ameri, 2017) reported that the TGA curve of the PDMS/PMHS shows a large weight loss between 250-375°C, indicating that the decomposition of the silicone structure occurs at temperatures higher than the investigated range. In addition, Hosseini and Tanaka (Hosseini and Ameri, 2017; Tanaka et al., 2010) attribute the slight weight loss up to 200°C to the removal of hexane and hydrogen formed by the reaction of PDMS and PHMS. The lack of any peaks in the first derivate signal, reported in Figure 4b, is a demonstration that the degradation process of the polymer is still starting, but it does not become relevant until 300°C. Indeed, it is worth pointing out that the range of temperatures in which the composite foam will be employed (25-130°C approximately) is not contained in the degradation range of the TG-measurements study, thus it is possible to assert that the pure foam is stable in the range of temperature needed for the application.

The thermal analysis of pure $MgSO_4 \cdot 7H_2O$ shows a significant sensitivity to the dehydration process with the increasing of temperature. In particular, analysing the curve, the dehydration process of the salt can be divided in three steps, each one accompanied by a peak showed in the first derivate signal in Figure 4b. Each dehydration step corresponds to the loss of one or more molecules of water. Going into more details:

- Stage I: The first dehydration step occurs between room temperature and 50°C, consisting of 6.45% mass loss; this stage can be related to the loss of a water molecule: the transition of $MgSO_4 \cdot 7H_2O$ to $MgSO_4 \cdot 6H_2O$ occurred. It is worth to note that this process already starts at about 25°C, indicating that the dehydration in magnesium sulphate hexahydrate is energetically favoured.
- Stage II: The second stage takes place between 50°C and 245°C. This stage is characterized by the largest mass loss (43.24%) in the studied range of temperatures.

  In this case, two dehydration sub-steps can be identified. The first consists of an abrupt reduction of mass weight and occurs between 50°C and 150°C. Vice versa, between 150°C and 245°C a more gradual reduction in mass loss takes place. In the first sub-step, a reduction of about 38.71% is calculated, indicating a loss of approximately 5.35 water molecules. A further weight loss of 4.53% was estimated in the second sub-step. Consequently, 0.62 water molecules are released in this case. Globally, this dehydration stage involves the transition from $MgSO_4 \cdot 6H_2O$ to $MgSO_4 \cdot 0.1H_2O$.

- Stage III: The last dehydration stage occurs between 245°C and 300°C and involves a mass loss of 0.95%, corresponding to about 0.1 water molecules. During the last stage, the transition to anhydrous $MgSO_4$ is completed.

The reported results are in close agreement with the data reported by van Essen (van Essen et al., 2009).

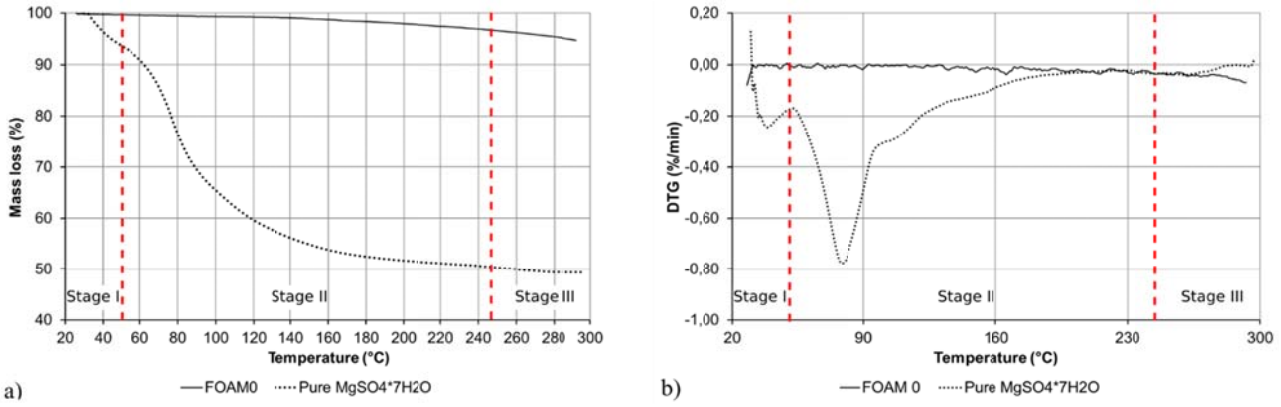

Figure 4. TGA measurement of unfilled foam: (a) mass loss percentage; (b) first derivate of TG-signal

3.2. Foam characterization

First, the evaluation of density and foam porosity was performed for all the synthetized foams. The main results are reported in Table 1.

Table 1. Main characteristics of the foams

	ρ_{foam} (g/cm^3)	$\rho_{salt\ hydrate}$ (g/cm^3)	ρ_{PDMS} (g/cm^3)	% salt hydrate	ρ_{bulk} (g/cm^3)	Foam porosity (%)
FOAM40	0.40	1.67	0.97	40%	1.25	68%
FOAM50	0.45			50%	1.32	66%
FOAM60	0.51			60%	1.39	63%
FOAM70	0.57			70%	1.46	61%

Bulk density was calculated applying the mixture rule on constituent content. The foam porosity was calculated using the equation:

$$Foam\ porosity = 1 - \frac{\rho_{foam}}{\rho_{bulk}}$$

Where ρ_{foam} and ρ_{bulk} are foam and composite density, respectively.

The results highlight that the density of the bulk grows with the increasing content of the salt hydrate, varying from 1.25g/cm^3 (FOAM40) to 1.46 g/cm^3 (FOAM70). The obtained values are always higher than the density of the pure silicone foam. Indeed, this last has a density equal to 0.28 g/cm^3, as reported by Calabrese et al. (Luigi Calabrese et al., 2017b). The foam porosity of the composite samples decreases with increasing salt content. Furthermore, the addition of salt in the formulation induces an increase in the density of the foamed structure (passing from 0.40g/cm^3 for FOAM40 up to 0.57g/cm^3 for FOAM70). This behaviour can be justified considering that the foam with lower salt content is characterized by better

foaming capacity. The salt, not actively participating in the foaming phase, acts as an inert filler in the chemical reaction between PDMS and PMHS, resulting in a lower efficacy on the increase in volume induced by the coupling dehydrogenative reaction. However, the achieved porosity level is in any case effective, and, as will be shown by optical microscopy images (Figure 6), the cellular microstructure of the foam is homogeneous even for samples with high contents of salt.

Figure 5 shows the FTIR spectrum of a composite foam (FOAM50). The large peak at about 1000 cm^{-1} is related to siloxane bond, due to the chemical reaction between hydroxyl group in PDMS and hydride groups in PMHS compounds. This broad peak overlaps the asymmetric and symmetric vibration peaks of SO_4 preventing a clear identification of the salt. However, the peak at about 620 cm^{-1} can be ascribed to the bending vibration of SO_4 groups of magnesium sulphate salt.

The effective and complete crosslinking of the composite foam is confirmed observing that the peaks of Si-OH (~680 cm^{-1}) and Si-H groups (~2100 cm^{-1}) are very depressed. This verifies that all reactive sites of PDMS and PMHS siloxane compounds chemically interacted together making a well cross-linked network. The broad absorption band at 3500 cm^{-1} and well defined peak at 1640 cm^{-1} can be assigned to stretching and bending modes, respectively, of hydroxyl groups of intracrystalline water in magnesium sulphate salt.

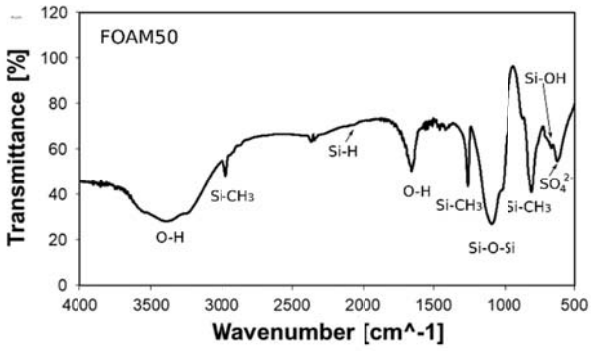

Figure 5. FTIR spectrum of FOAM50

The optical microscope, equipped with a high-resolution photo-camera, was used to investigate the pore distribution as well as the homogeneity of the salt dispersed inside the structure. Figure 6 shows the cross section of the samples at various salt contents along foaming direction. The pictures highlight that the foams show very similar morphology regardless of the amount of hydrated salt added. All foam samples, characterized by spheroidal shaped cells, present a mixed open/closed cell structure. The bubbles appear homogeneously distributed along the cross section and they are well interconnected each other, so that the water vapour can easily diffuse inside the porous structure.

Even though the foams show a mixed open/close cell structure, PDMS has a high permeability to water vapour (Robb, 1968; Shui Wai Lin and Salvador Valera Lamas, 2011) that assures a good diffusion of the water vapour also inside the closed cell, where the grains of the salt hydrate could be embedded, producing a permeable structure characterized by excellent sorption performance.

Figure 6. Optical microscopy photos of filled foams at various percentage

As mentioned before, Figure 6 highlights that increasing the salt content causes a reduction of foam ability. In other words, it is observed a slightly lower foam porosity especially for the higher amount of salt – see Table 1, i.e. FOAM70, it influences the flexibility of the composite porous structure, due to the reduction of the polymeric matrix itself.

The magnification of the pore structure reported in Figure 7 evidences that when the amount of the salt is low (i.e. 40 wt.%), small size granules of the hydrated salt (i.e. about 5 μm) are confined inside the pores; instead, the polymeric foam is totally covered by grains of salt when high percentages are added (i.e. 70 wt.%). This can be justified by the limited percentage of polymeric foam, which, probably, during the foaming process is not able to homogenously embed all the salt grains.

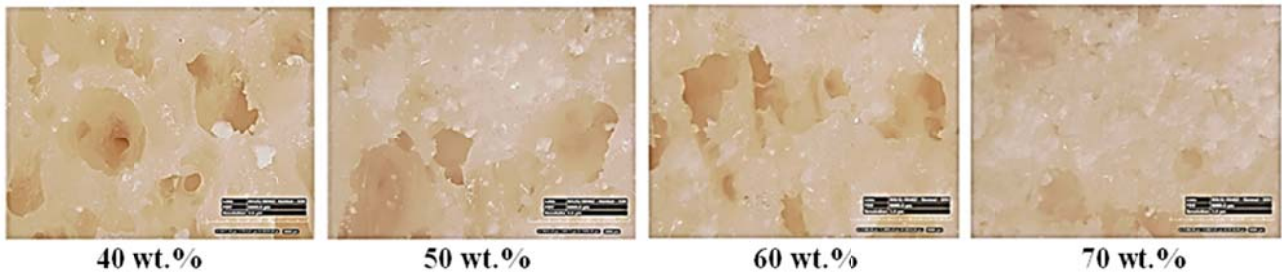

Figure 7. Magnification of porous structure of filled foams at various percentage

It has to be pointed out that, differently from the composites employing zeolite as filler (Luigi Calabrese et al., 2017b), only physical links take place between the salt powder and the polymeric foam. Thus, the salt is confined and constrained inside the porous structure. Scanning Electron Microscopy (SEM) analysis was performed to carefully analyse the distribution of salt inside the foam. Figure 8 shows the micrograph, at magnification of 800x, of sample FOAM40. EDS spectra, obtained on the pure matrix and on the grain of salt hydrate found in the area, are reported in the same figure.

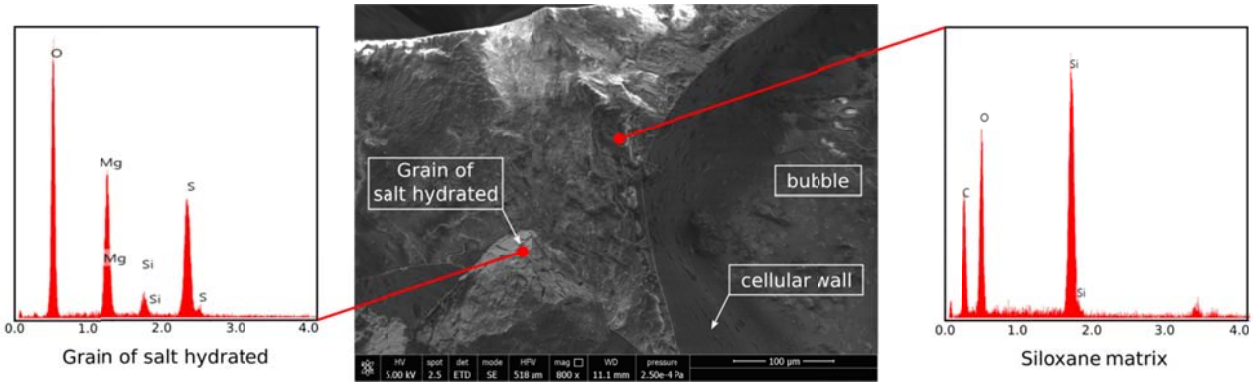

Figure 8. Micrograph and EDS spectra of FOAM40 sample

The micrograph shows a grain of salt hydrate covered by the matrix and well embedded in it, confirming that the salt hydrate is well adherent to the silicone foam. Foam walls cross sections are homogenous without voids or micro cracks indicating a good interconnection between salt hydrate and polymer matrix. However, the effective filmogeneity of the siloxane matrix allowed sometimes the formation of a coating layer on the salt hydrate, which in this way is encapsulated in the structure reducing the risk of removal during handling of the composite foam. The EDS spectra, evaluated in two different points of the samples, highlight that the characteristic elements of the matrix is still present on the grain of salt hydrate covered by the matrix, as confirmed by silicon peak due to siloxane compounds.

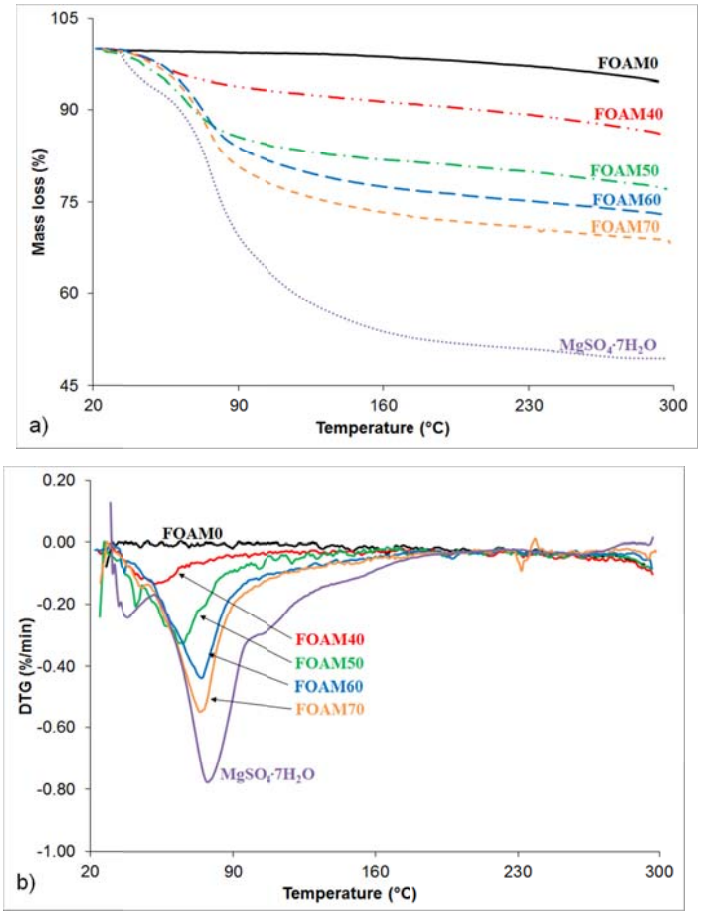

Figure 9. TGA measurement of the foams: a) mass loss percentage b) first derivate of TG-signal

TGA investigation was used to analyse the dehydration behaviour of the composite foams with increasing temperature. The experimentation on the main constituents of the foam (showed in Figure 4) highlighted that the salt is characterized by the most consistent mass loss in the investigated range of temperatures. TGA results of the composite foams, showed in Figure 9, reveal that, increasing the amount of the salt hydrate inside the matrix, the behaviour of the foams is more comparable with that of the pure salt. Anyway, it is evident that the mass loss (see Figure 9a) is not proportional to the percentage of the salt inside the matrix. In particular, the pure salt hydrate evidenced a mass loss of 50.65%. Instead, FOAM 40 and FOAM 70 showed a mass loss of 13.86% and 31.10%, respectively, indicating that the composite foams exhibited dehydration performances slightly less effective that the theoretical one. One possible reason for this behaviour is that a a previous lightly dehydration of the salt hydrate occurred during the preparation step at 60°C for 24h of the foams. Nevertheless, another experimental evidence is that handling the foams produces a slightly loss of the salt hydrate filler. Anyway, as evidenced before, the lower is the salt content the better is the embedding efficiency inside the matrix; for higher content of salt hydrate, an effective linking of the salt to the matrix is more difficult and the loss is higher.

Further details on dehydration process can be assessed analysing the mass loss trend at increasing temperature for all samples. Excluding the pure siloxane foam (FOAM0) all composite foams samples evidenced two evident mass drop (Figure 9a) at low and medium temperature, respectively. Initially, at about 30°C, a small mass reduction can be identified. This transition, similarly to the interpretation proposed for

the pure hydrate, is ascribed to loss of a single water molecule in the salt hydrate. Afterwards, in the temperature range of about 60-180°C a significant loss in weight can be identified, due to a larger loss of intracrystalline water from the salt hydrate. Also the first derivate of the TG-signal (see Figure 9b) highlights the weight loss phenomena related to the increasing temperature. Indeed, two peaks can be clearly identified in the graph. The first peak remains approximately constant for all samples (from the pure salt to the composite foams). Vice versa, the second peak moves to higher temperatures increasing the amount of salt hydrate. This phenomenon depends from the amount of water that comes out from the samples higher is the quantity of released water higher is the peak temperature. In any case, the on set temperature of these peaks seems to be constant regardless the amount of the filler embedded in the matrix and approximately equals to 30°C.

In order to assess the ability of the synthetized composites foam-salt to properly react with water vapour, under typical working conditions, thermo-gravimetric dehydration tests were performed. The results of the performed tests are reported in Figure 10. In particular, the pure salt was tested as reference, showing a mass loss of about 45% at 150°C, corresponding to about 6 water molecules released. To understand the behaviour of the pure polymeric foam, also FOAM0 sample was tested as reference. It showed a negligible weight loss in the range of investigated temperatures.

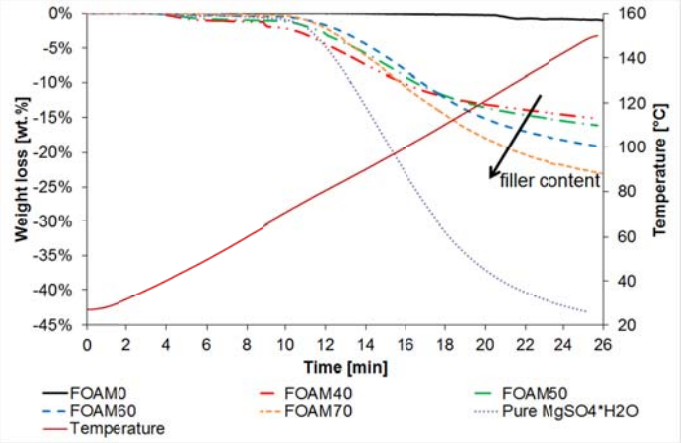

Figure 10. Thermo-gravimetric dehydration measurements in presence of water vapour at 23.4 mbar of unfilled and filled samples

In order to calculate the mass loss for the composite samples, the reference salt mass was taken considering the nominal salt content of each sample. As reported in Figure 10, none of the tested samples reaches the expected mass loss quantity of the pure salt, demonstrating that the actual salt content for each composite is lower than expected. Starting from the water mass loss, measured for each tested sample, it was possible to calculate the actual salt content.

Table 2 summarizes the performed calculations, as average of the three experiments on three different pieces of foam for each sample. It is evident that the spread between the nominal salt content and actual salt content is always less than 10%, except for sample FOAM70 where the spread reaches a higher value. The obtained results can be caused by the following experimental issues:

- partial dissolution of the salt inside the solvent during the foam preparation phase;

- loss of salt during the handling of the samples; and
- incomplete incorporation of the salt inside the foam during the foaming process, due to the incomplete foaming process induced by the excessive amount of salt employed.

Table 2: Water mass loss measured during the performed tests and actual salt content calculated for each tested samples.

Sample	Initial mass sample (mg)	Total weight loss (mg)	Nominal salt content [wt.%]	Water mass loss [wt.%]	Actual salt content [wt.%]
Pure $MgSO_4 \cdot 7H_2O$	37.39	16.4	100	43.90	100
FOAM40	52.62	8.7	40	41.29	37.15
FOAM50	96.86	17.7	50	36.50	41.08
FOAM60	110.87	28.1	60	42.02	56.74
FOAM70	90.37	23.6	70	37.05	58.37

Summing up the results obtained from the experimental campaign on the silicone foams added with $MgSO_4 \cdot 7H_2O$, it is possible to assert that the amount of salt hydrate, that can be added to the matrix, have to be carefully evaluated because it was observed that high amount of filler does not assure a correct embedding in the matrix. The hypothesis that a salt hydrate threshold value, approximately 60%, beyond which the silicone matrix is not able to efficiently incorporate salt hydrate, is highly credible. Furthermore, the foams with lower amount of salt hydrate (FOAM40 – FOAM50) show a better foam capability that assures also a high flexibility of the composite porous structure. Nevertheless, they clearly show lower dehydration ability than the sample with a higher content of filler (FOAM60 – FOAM70). Therefore, once again, the foam realized with an amount of filler of around 60% seems to be a good compromise between foam ability, flexibility and de/hydration capacity.

Regarding the thermal energy storage applications, the results indicated a sensibility to the salt content in terms of de/hydration behavior in a range of over 20 K, with an increasing tendency to release water molecules at high temperature for a higher salt content. Such an aspect is of great interest for thermal energy storage applications, foreseeing the possibility of tailoring the material for each specific application (i.e. charge/discharge temperature requirement) by simply changing the amount of salt within the composite. Finally, since a good link seems to be established between the foam and the salt, and that the de/hydration capacity of the salt is not hindered by the foaming process, storage ability and storage density of the composites are expected to be in line with those of the pure material.

4. Conclusions

The paper deals with innovative composite sorbents for sorption storage applications, realised by embedding $MgSO4 \cdot 7H_20$ inside a polymeric matrix. The polymeric material, made by a mixture of poly(methylhydrosiloxane) $(CH_3(H)SiO)_n$ and a silanol terminated polydimethylsiloxane with proper catalyst, was employed to form a polymeric foam that represents the hosting matrix for the salt hydrate,

$MgSO_4 \cdot 7H_2O$, which was chosen for its excellent sorption capacity. The polymers were selected for their high permeability to water vapour, in order not to affect the water vapour diffusion during real operating conditions.

Foams with various salt hydrate percentages (from 40 wt.% to 70 wt.%) were investigated, by means of: FTIR analysis that has demonstrated that all reactive sites of PDMS and PMHS siloxane compounds chemically interacted together making a well cross-linked network. Morphological analysis has evidenced that the morphology of the foam samples does not depend on the amount of filler and is characterized by spheroidal shaped cells, producing a mixed open/closed cell structure with bubbles homogeneously distributed along the cross section well interconnected each other, so that, the water vapour can easily diffuse inside the porous structure. SEM microscopy has revealed that the salt is confined and constrained inside the porous structure; and, finally, the study of the dehydration process of the salt inside the foam has permitted to suppose that a salt hydrate threshold value, approximately 60%, exists beyond which the silicone matrix is not able to efficiently incorporate salt hydrate. Indeed, the foam realized with an amount of filler of around 60% seems to be a good compromise between foam ability, flexibility and de/hydration capacity.

Regarding the thermal energy storage applications, the results indicated a sensibility to the salt content in terms of de/hydration behavior in a range of over 20 K, with an increasing tendency to release water molecules at high temperature for a higher salt content. It is then possible to conclude that the investigated composite foams can represent a promising candidate for thermal energy storage applications.

Acknowledgements

The present work has been partially funded by PON “Ricerca e Competitività 2007-13” PON03PE_00206_2 S5 - Smart Small Scale Solar Systems and by the Spanish government (ENE2015-64117-C5-1-R (MINECO/FEDER)). The authors from the University of Lleida would like to thank the Catalan Government for the quality accreditation given to their research group (2014 SGR 123). Aran Solé would like to thank Ministerio de Economía y Competitividad de España for Grant Juan de la Cierva, FJCI-2015-25741.

References

Aydin, D., Casey, S.P., Riffat, S., 2015. The latest advancements on thermochemical heat storage systems. Renew. Sustain. Energy Rev. 41, 356–367. doi:10.1016/J.RSER.2014.08.054

Cabeza, L.F., Solé, A., Barreneche, C., 2017. Review on sorption materials and technologies for heat pumps and thermal energy storage. Renew. Energy 110, 3–39. doi:10.1016/j.renene.2016.09.059

Calabrese, L., Bonaccorsi, L., Bruzzaniti, P., Freni, A., Proverbio, E., 2018. Morphological and functional aspects of zeolite filled siloxane composite foams. J. Appl. Polym. Sci. 135. doi:10.1002/app.45683

Calabrese, L., Bonaccorsi, L., Bruzzaniti, P., Gullì, G., Freni, A., Proverbio, E., 2017a. Zeolite filled siloxane

composite foams: Compression property. J. Appl. Polym. Sci. doi:10.1002/app.46145

Calabrese, L., Bonaccorsi, L., Freni, A., Proverbio, E., 2017b. Silicone composite foams for adsorption heat pump applications. Sustain. Mater. Technol. 12, 27–34. doi:10.1016/J.SUSMAT.2017.04.002

Calabrese, L., Bonaccorsi, L., Freni, A., Proverbio, E., 2017. Synthesis of SAPO-34 zeolite filled macrocellular foams for adsorption heat pump applications: A preliminary study. Appl. Therm. Eng. 124, 1312–1318. doi:10.1016/j.applthermaleng.2017.06.121

Courbon, E., D'Ans, P., Permyakova, A., Skrylnyk, O., Steunou, N., Degrez, M., Frère, M., 2017. Further improvement of the synthesis of silica gel and CaCl2 composites: Enhancement of energy storage density and stability over cycles for solar heat storage coupled with space heating applications. Sol. Energy 157, 532–541. doi:10.1016/J.SOLENER.2017.08.034

De Jong, A.-J., Trausel, F., Finck, C., Van Vliet, L., Cuypers, R., 2014. Thermochemical heat storage – system design issues. Energy Procedia 48, 309–319. doi:10.1016/j.egypro.2014.02.036

Donkers, P.A.J., Pel, L., Adan, O.C.G., 2016. Experimental studies for the cyclability of salt hydrates for thermochemical heat storage. J. Energy Storage 5, 25–32. doi:10.1016/j.est.2015.11.005

Donkers, P.A.J., Sögütoglu, L.C., Huinink, H.P., Fischer, H.R., Adan, O.C.G., 2017. A review of salt hydrates for seasonal heat storage in domestic applications. doi:10.1016/j.apenergy.2017.04.080

Frazzica, A., Sapienza, A., Freni, A., 2014. Novel experimental methodology for the characterization of thermodynamic performance of advanced working pairs for adsorptive heat transformers. Appl. Therm. Eng. 72, 229–236. doi:10.1016/J.APPLTHERMALENG.2014.07.005

Gaeini, M., Rouws, A.L., Salari, J.W.O., Zondag, H.A., Rindt, C.C.M., 2018. Characterization of microencapsulated and impregnated porous host materials based on calcium chloride for thermochemical energy storage. Appl. Energy 212, 1165–1177. doi:10.1016/j.apenergy.2017.12.131

Genceli, F.E., Lutz, M., Spek, A.L., Witkamp, G.J., 2007. Crystallization and characterization of a new magnesium sulfate hydrate MgSO4 11H2O. Cryst. Growth Des. 7, 2460–2466. doi:10.1021/cg060794e

Gordeeva, L.G., Aristov, Y.I., 2012. Composites "salt inside porous matrix" for adsorption heat transformation: a current state-of-the-art and new trends. Int. J. Low-Carbon Technol. 7, 288–302. doi:10.1093/ijlct/cts050

Hongois, S., Kuznik, F., Stevens, P., Roux, J.-J., 2011. Development and characterisation of a new MgSO4−zeolite composite for long-term thermal energy storage. Sol. Energy Mater. Sol. Cells 95, 1831–1837. doi:10.1016/j.solmat.2011.01.050

Hosseini, M., Ameri, E., 2017. Pervaporation characteristics of a PDMS/PMHS membrane for removal of

dimethyl sulfoxide from aqueous solutions. Vacuum 141, 288–295. doi:10.1016/j.vacuum.2017.04.032

International Energy Agency, 2013. Transition to sustainable buildings - Strategies and Opportunities to 2050.

Jabbari-Hichri, A., Bennici, S., Auroux, A., 2017. CaCl2-containing composites as thermochemical heat storage materials. Sol. Energy Mater. Sol. Cells 172, 177–185. doi:10.1016/J.SOLMAT.2017.07.037

Jänchen, J., Ackermann, D., Stach, H., Brösicke, W., 2004. Studies of the water adsorption on Zeolites and modified mesoporous materials for seasonal storage of solar heat. Sol. Energy 76, 339–344. doi:10.1016/J.SOLENER.2003.07.036

Kerskes, H., Mette, B., Asenbeck, S., Drück, H., Müller-Steinhagen, H., 2010. Experimental and Numerical investigations on Thermo-Chemical Heat Storage. EuroSun 1–10.

Kleiner, F., Posern, K., Osburg, A., 2017. Thermal conductivity of selected salt hydrates for thermochemical solar heat storage applications measured by the light flash method. Appl. Therm. Eng. 113, 1189–1193. doi:10.1016/J.APPLTHERMALENG.2016.11.125

Liu, H., Nagano, K., Togawa, J., 2015. A composite material made of mesoporous siliceous shale impregnated with lithium chloride for an open sorption thermal energy storage system. Sol. Energy 111, 186–200. doi:10.1016/J.SOLENER.2014.10.044

Miao, K., Lu, Z., Cao, J., Zhang, H., Li, D., 2016. Effect of polydimethylsiloxane on the mid-temperature strength of gelcast Al2O3 ceramic parts. Mater. Des. 89, 810–814. doi:10.1016/j.matdes.2015.09.150

Mrowiec-Białoń, J., Jarzębski, A.B., Lachowski, A.I., Malinowski, J.J., Aristov, Y.I., 1997. Effective Inorganic Hybrid Adsorbents of Water Vapor by the Sol-Gel Method. Chem. Mater. 9, 2486–2490. doi:10.1021/cm9703280

Posern, K., Kaps, C., 2010. Calorimetric studies of thermochemical heat storage materials based on mixtures of MgSO4 and MgCl2. Thermochim. Acta 502, 73–76. doi:10.1016/j.tca.2010.02.009

Ramalingom, S., Podder, J., Kalkura, S.N., Bocelli, G., 2003. Habit modification of epsomite in the presence of urea. J. Cryst. Growth 247, 523–529. doi:10.1016/S0022-0248(02)01991-7

Rammelberg, H.U., Osterland, T., Priehs, B., Opel, O., Ruck, W.K.L., 2016. Thermochemical heat storage materials – Performance of mixed salt hydrates. Sol. Energy 136, 571–589. doi:10.1016/J.SOLENER.2016.07.016

RHC European Technology Platform, 2014. Solar Heating and Cooling Technology Roadmap.

Ristić, A., Henninger, S.K., 2014. Sorption Composite Materials for Solar Thermal Energy Storage. Energy

Procedia 48, 977–981. doi:10.1016/J.EGYPRO.2014.02.111

Robb, W.L., 1968. Thin silicon membranes. Their permeation properties and some applications. Ann. N. Y. Acad. Sci. 146, 119–137. doi:10.1111/j.1749-6632.1968.tb20277.x

Shui Wai Lin and Salvador Valera Lamas, 2011. Air Dehydration by Permeation Through Dimethylpolysiloxane/polysulfone Membrane. J. Mex. Chem. Soc. 55, 42–50.

Silverstein, R.M., Webster, F.X., Kiemle, D., Einholm, E.J., 2005. Spectrometric Identification of Organic Compounds, 7th Edition. J. Magn. Reson. Ser. A. doi:10.1006/jmra.1996.0145

Tanaka, S., Chao, Y., Araki, S., Miyake, Y., 2010. Pervaporation characteristics of pore-filling PDMS/PMHS membranes for recovery of ethylacetate from aqueous solution. J. Memb. Sci. 348, 383–388. doi:10.1016/j.memsci.2009.11.033

van Essen, V.M., Zondag, H.A., Gores, J.C., Bleijendaal, L.P.J., Bakker, M., Schuitema, R., van Helden, W.G.J., He, Z., Rindt, C.C.M., 2009. Characterization of MgSO[sub 4] Hydrate for Thermochemical Seasonal Heat Storage. J. Sol. Energy Eng. 131, 41014. doi:10.1115/1.4000275

Whiting, G., Grondin, D., Bennici, S., Auroux, A., 2013. Heats of water sorption studies on zeolite-MgSO4 composites as potential thermochemical heat storage materials. Sol. Energy Mater. Sol. Cells 112, 112–119. doi:10.1016/j.solmat.2013.01.020

Whiting, G.T., Grondin, D., Stosic, D., Bennici, S., Auroux, A., 2014. Zeolite–MgCl2 composites as potential long-term heat storage materials: Influence of zeolite properties on heats of water sorption. Sol. Energy Mater. Sol. Cells 128, 289–295. doi:10.1016/J.SOLMAT.2014.05.016

Xu, C., Yu, Z., Xie, Y., Ren, Y., Ye, F., Ju, X., 2018. Study of the hydration behavior of zeolite-MgSO 4 composites for long-term heat storage. Appl. Therm. Eng. 129, 250–259. doi:10.1016/j.applthermaleng.2017.10.031

Xu, J., Wang, R.Z., Li, Y., 2014. A review of available technologies for seasonal thermal energy storage. Sol. Energy 103, 610–638. doi:10.1016/j.solener.2013.06.006

Yu, N., Wang, R.Z., Wang, L.W., 2013. Sorption thermal storage for solar energy. Prog. Energy Combust. Sci. 39, 489–514. doi:10.1016/j.pecs.2013.05.004

Zhao, Y.J., Wang, R.Z., Zhang, Y.N., Yu, N., 2016. Development of SrBr2 composite sorbents for a sorption thermal energy storage system to store low-temperature heat. Energy 115, 129–139. doi:10.1016/j.energy.2016.09.013

Zhu, D., Wu, H., Wang, S., 2006. Experimental study on composite silica gel supported CaCl2 sorbent for low grade heat storage. Int. J. Therm. Sci. 45, 804–813. doi:10.1016/j.ijthermalsci.2005.10.009

1